Journal of Magnetic Resonance **139,** 454–459 (1999)
Article ID jmre.1999.1808, available online at http://www.idealibrary.com on IDEAL®

Band-Selective HSQC and HMBC Experiments Using Excitation Sculpting and PFGSE

Christine Gaillet, Christelle Lequart,* Philippe Debeire,* and Jean-Marc Nuzillard[1]

*Laboratoire de Pharmacognosie, UPRES-A 6013, Moulin de le Housse, 51097 Reims Cedex 2, France; and *Laboratoire de Fractionnement Enzymatique, UPBP, Institut National de la Recherche Agronomique, Moulin de la Housse, BP 1039, 51687 Reims Cedex 2, France*

Received February 17, 1999; revised April 27, 1999

Variants of the HSQC and HMBC experiments are described. They allow the restriction of the heteronuclear chemical shift domain without causing spectral folding. Selectivity is introduced in the HSQC experiment by means of excitation sculpting. The selective element of the pulse sequence is a double pulsed field gradient spin echo. It may be used either split by the t_1 evolution period, or not. The selectivity profile depends on the scheme used as well as on the number of protons attached to the heteronucleus. The selective HMBC experiment requires only a single echo sequence as no strict control of the signal phase is required. A complex glycoconjugate is used as a test compound for the new pulse sequences. © 1999 Academic Press

Key Words: **excitation sculpting; heteronuclear chemical shift correlation; selective pulses; NMR; glycoconjugates.**

HMBC and HSQC experiments play a key role in structural elucidation of organic molecules. They offer a rich information content and a sensitivity that makes them useful in the resolution of a wide range of structural problems (*1*). When the complexity of the studied molecules increases, the resolution in the F_1 domain becomes of critical importance. Even in simple molecules one can often find one or more couples of ^{13}C resonances that cannot be separated in 2D inverse correlation maps. Data processing techniques such as linear prediction (*2*) or filter diagonalization (*3*) exploit at best the available resolution through time domain signal modeling.

The F_1 resolution, defined by the ratio of the number of t_1 increments to the F_1 spectral width, is proportional to the width of the explored t_1 domain, referred to as t_{1max}. Therefore, a better resolution can be obtained by an increase in the number of t_1 increments. The enhancement applies to the whole F_1 domain, even where not required. Alternatively, the reduction of the F_1 spectral width achieves the desired goal while keeping the number of t_1 increments at a practical value. The main drawback of this approach is the folding of the resonance peaks lying outside of the chosen spectral domain. The clean reduction of the F_1 spectral domain is achieved by selective pulses that cover the desired frequency range of indirectly detected resonance frequencies (*4–8*). The resolution cannot be indefinitely improved because it is limited by relaxation during t_1. An increase of t_{1max} leads thus to a decrease of the signal-to-noise ratio if the overall recording time is kept constant. This is the price to pay for the resolution enhancement. This Communication shows how gradient-enhanced HSQC and HMBC pulse sequences can incorporate excitation sculpting and PFGSE in order to achieve F_1 band-selective experiments.

Excitation sculpting (*9*) is produced by the application of a double pulsed field gradient spin-echo sequence (DPFGSE). The spin echoes are induced by selective inversion pulses *S*. The sequence *S* needs only to be characterized by its inversion profile $M_{zz}(\Omega)$. This is the amount of *z* magnetization that is recovered after the action of the pulse on a nucleus of offset frequency Ω, starting from its equilibrium state. A derived quantity of interest is the inversion probability $P(\Omega) = (1 - M_{zz}(\Omega))/2$. The DPFGSE sequence preserves the phase of the incoming transverse magnetization and modulates its amplitude according to $A(\Omega) = P^2(\Omega)$.

The nonselective pulse sequence in Fig. 1a was retained to show how the DPFGSE element can be introduced in a gradient-enhanced HSQC experiment (*10*). The coherence transfer pathway simultaneously selects $p = +1$ and $p = -1$ states of *X* during t_1. This creates amplitude-modulated signals that allow a quadrature detection scheme in F_1 by the TPPI method. The pulse sequence in Fig. 1b shows the straight insertion of the DPFGSE element in the corresponding nonselective experiment. The latter was chosen so that there is no spatial labeling of magnetization before t_1, thus avoiding signal loss by diffusion if long t_1 periods are used (*11*). The intrinsic selectivity profile is modified by the action of one or more heteronuclear couplings. Interestingly, $A(\Omega)$ can still be expressed by means of the inversion probability function *P* in the absence of coupling. The analytical expressions of $A(\Omega)$ make use of the probabilities

$$P_n = P(\Omega_X + n\pi J) \quad [1]$$

[1] To whom correspondence should be addressed. E-mail: jm.nuzillard@univ-reims.fr. Fax: 33 3 26 05 35 96.

1090-7807/99 $30.00

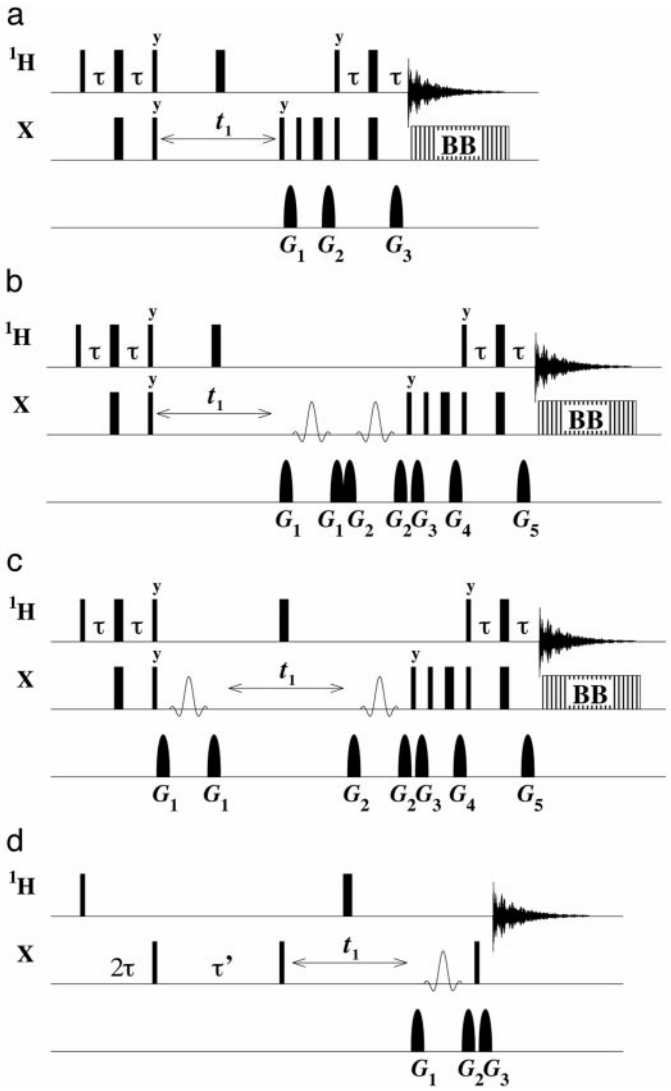

FIG. 1. In all pulse sequences thin and thick vertical black bars indicate $\pi/2$ and π pulses, respectively. Pulse phases are x unless otherwise specified. Delays τ equal $\frac{1}{4}J(X\mathrm{H})$. (a) The basic nonselective pulse sequence of the gradient-enhanced HSQC experiment, using TPPI for quadrature detection in F_1. (b) Straight introduction of a DPFGSE in sequence (a). (c) Alternative X-selective pulse sequence in which the spin echoes are separated by the t_1 period. (d) Introduction of a PFGSE sequence in the HMBC experiment. τ' is the action time of long-range X–H couplings.

in which Ω_X is the X offset and J the involved coupling constant. The incoming magnetization is described by the operator I_zS_+. The density matrix calculation of the resulting I_zS_+ term is carried out in a way similar to that exposed in Ref. (*9*). The state of the X spin is described in the (S_+, S_-, S_z) basis set, and the state of the ^{1}H spins is written in the population operators basis. The Hamiltonian operator that acts during the soft pulses is expressed as a sum of single transition operators (*12*). These choices allow an easy tracing of the magnetization evolution during the DPFGSE sequence, leading to

$$\begin{aligned} X\mathrm{H}\text{ group:}\quad & A(\Omega_X) = (P_1^2 + P_{-1}^2)/2 \\ X\mathrm{H}_2\text{ group:}\quad & A(\Omega_X) = (P_2^2 + 2P_0^2 + P_{-2}^2)/4 \\ X\mathrm{H}_3\text{ group:}\quad & A(\Omega_X) = (P_3^2 + 3P_1^2 + 3P_{-1}^2 + P_{-3}^2)/8. \end{aligned} \quad [2]$$

In these expressions, $A(\Omega_X)$ appears to be the convolution product of $P^2(\Omega)$ by the shape of the X multiplet. Each line of the multiplet may indeed be considered separately as being produced by a fictitious uncoupled nucleus of offset frequency $\Omega_X + n\pi J$. The intensity of each line is then independently modulated by the DPFGSE sequence according to the P^2 function. The effect produced is clearly visible when the width of the selectivity profile is less than J. However, band-selective experiments are not intended to be employed in such a limit situation.

Symmetry in the pulse sequence can be restored by setting a PFGSE before t_1 and the other one after t_1, as shown in Fig. 1c. The presence of an X inversion pulse before t_1 inverts the apparent evolution frequency of the X magnetization. The TPPI procedure is modified accordingly by changing the sign of the phase increment. The separation of the two echoes also affects the selectivity profile. The inversion pulse in the middle of t_1 exchanges the ^{1}H α and β states. A new variable ϕ is then needed to express $A(\Omega)$. A soft pulse acting on uncoupled nuclei rotates the magnetization around an axis located by means of the spherical coordinates θ and ϕ. In general, both depend on the offset and on the intensity and phase of the B_1 field. For constant phase pulses, ϕ is simply this phase angle. Angles ϕ_n and derived coefficients $c_{n,m}$ are defined for coupled nuclei by

$$\phi_n = \phi(\Omega_X + n\pi J) \quad [3]$$

$$c_{n,m} = \cos 2(\phi_n - \phi_m). \quad [4]$$

The theoretical selectivity profile is then

$$\begin{aligned} X\mathrm{H}\text{ group:}\quad & A(\Omega_X) = -(P_1P_{-1}c_{1,-1}) \\ X\mathrm{H}_2\text{ group:}\quad & A(\Omega_X) = -(P_2P_{-2}c_{2,-2} + P_0^2)/2 \\ X\mathrm{H}_3\text{ group:}\quad & A(\Omega_X) = -(P_3P_{-3}c_{3,-3} + 3P_1P_{-1}c_{1,-1})/4. \end{aligned} \quad [5]$$

The minus sign appears because an I_zS_+ state is transformed into $-I_zS_+$ by the $\pi_x(I)$ pulse. The result in Eq. [5] may be found as well by individually considering the lines of a multiplet, taking into account the label inversion of the

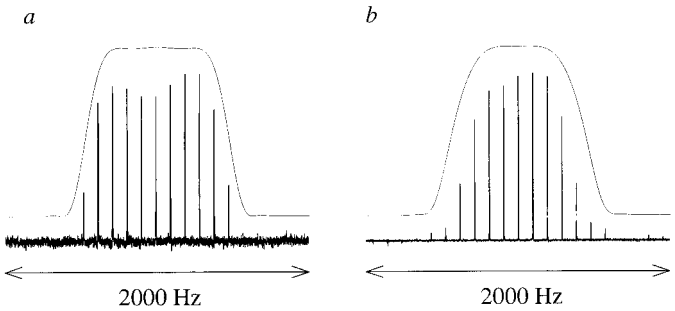

FIG. 2. Experimental determination of the selectivity profile achieved by the pulse sequence in Fig. 1c, restricted to the recording of the first t_1 value. All spectra are recorded on a Bruker DRX 500 spectrometer fitted with an inverse mode probe able to produce static field gradients up to 50 G · cm^{-1} along the *z* axis. The compound is 2,3,4,6-acetyl-1-methoxy-α-glucopyranose. Gradient strengths G_1, G_2, G_3, G_4, and G_5 are 35.5, 19, 15, 40, and 10 G · cm^{-1}. Gradient pulses are modulated by an arch of sine function; they last 1.2 ms and are followed by a 0.1-ms recovery delay. The selective inversion is ensured by a RE-BURP pulse 5 ms long, covering a 1000-Hz bandwidth. The *X* offset is incremented by 100-Hz steps between subplots. The subplot in the middle of each series corresponds to an on-resonance inversion. Continuous lines are theoretical selectivity profiles, computed according to Eq. [5]. (a) Test on the anomeric CH group. (b) Test on the CH_3 group.

^{1}H spin states induced by the hard inversion pulse. The coefficients $c_{n,m}$ equal 1 if ϕ is independent of the offset, like for a constant phase pulse. If the bandwidth is much smaller than *J*, then only the XH_2 groups respond (with half intensity) because both P_1P_{-1} and P_3P_{-3} cannot be significantly different from 0. Equations [2] and [5] were checked numerically using a brute force density matrix treatment in which the effect of gradient pulses was evaluated at different positions within the sample. The resulting spin state was calculated as the mean value of the terms of interest over the sample.

Figure 2 provides an experimental determination of selectivity profiles and a comparison of the result with theory. It is obtained by the 1D version of the pulse sequence in Fig. 1c when t_1 has its minimum value. It uses a RE-BURP pulse (*13*) applied to a CH carbon (Fig. 2a) and to a CH_3 carbon (Fig. 2b). The result is not as neat as expected, probably due to nonlinearities of the shaped pulse modulator in the decoupler channel. However, a slight "melting" of the selectivity profile is observed in Fig. 2b, caused by the presence of three direct heteronuclear couplings. The same 1D pulse sequence is employed in the calibration of the soft inversion pulse, even though other methods might be employed (*14*). The technique of spectral restriction used in the pulse sequences in Figs. 1b and 1c applies to other HSQC-related schemes, like the sensitivity-enhanced PEP-HSQC (*15*).

The F_1 band-selective HMBC (*16*) experiment does not require systematic refocusing of the ^{1}H magnetization. Proton multiplets are indeed distorted at the beginning of the pulse sequence, during the delay required by the production of *X*-coupled magnetization (*17*). The proposed pulse sequence is shown in Fig. 1d. It is designed to achieve phase modulation during t_1. Attempts to create amplitude-modulated data sets produces cross-shaped correlations as already described in Ref. (*18*). The benefit of resolution enhancement would then be partly lost, due to an increase in the probability of correlation peak superimposition. As in the HSQC experiment, the application of gradient pulses was avoided before t_1 in order to preserve the signal from diffusion effect. The second gradient pulse of the PFGSE is combined with the first gradient pulse required for the coherence pathway selection, resulting in a rather simple pulse sequence.

Feruloylarabinoxylane, **1** (see Fig. 3), isolated from wheat bran, presents very close ^{13}C resonance lines around 76 ppm. They correspond to the carbon atoms at positions C-2, C-3, and C-4 of the xylose units. The ferulic acid part is present as both the *cis* and *trans* forms, leading to two sets of chemical shifts in the arabinose residue. The reducing xylose is also present as a mixture of the α and β forms. Nonselective HSQC and HMBC spectra are drawn in Figs. 4a and 5a. The spectra in Figs. 4b and 5b present the F_1-selective HSQC and HMBC spectra recorded according to pulse sequences in Figs. 1c and 1d, respectively. The resolution improvement is particularly impressive in the HSQC spectrum. The rapid decay rate of the signals upon t_1 increase in the HMBC spectrum limits the highest resolution

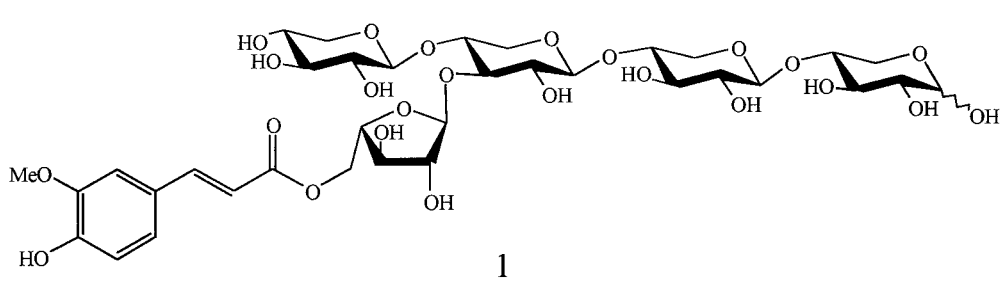

1

FIG. 3. The structure of the test compound, feruloylarabinoxylane, extracted from wheat bran.

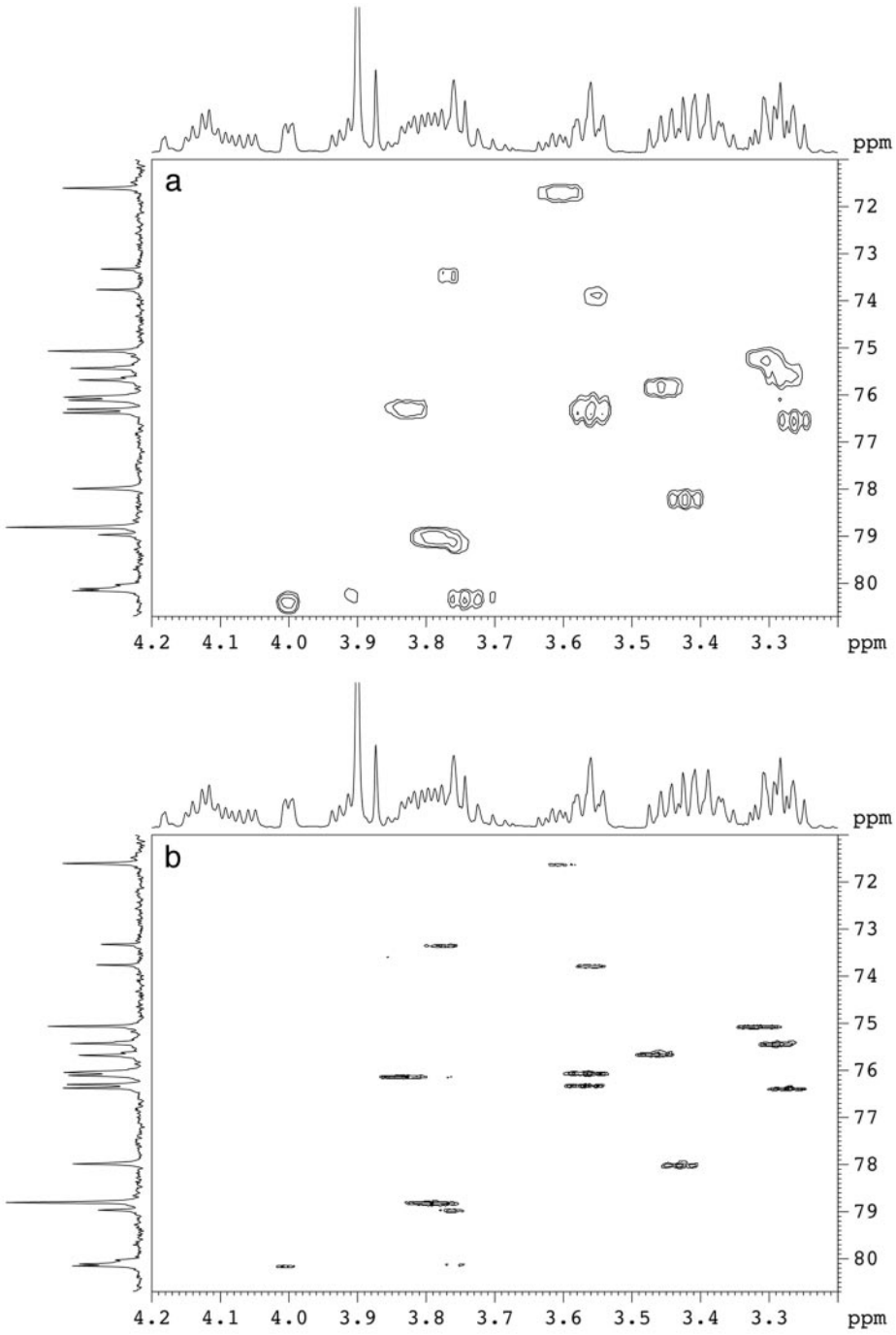

FIG. 4. (a) The ^{1}H–^{13}C HSQC spectrum of compound **1**. The sample (15 mg) is dissolved in 0.7 mL D_2O. The total spectral width in F_1 is 160 ppm, with 512 t_1 increments (t_{1max} = 25 ms). Only the zone around 76 ppm is displayed. Gradient strengths G_1, G_2, and G_3 are 15, 40, and 10 G · cm^{-1}. Sixteen scans were used per t_1 value, resulting in an overall recording time of 2.8 h. (b) The F_1-selective HSQC spectrum of compound **1**, recorded with the pulse sequence in Fig. 1c. The selective inversion is ensured by a RE-BURP pulse 5 ms long, as for the spectra in Fig. 2. The total spectral width in F_1 is 10 ppm, with 256 t_1 increments (t_{1max} = 204 ms). Thirty-two scans were used per t_1 value, resulting in an overall recording time of 4.0 h. The TPPI procedure requires the phase decrementation of the first $\pi/2(X)$ pulse at each t_1 change.

that can be achieved. Greater t_{1max} values would only deteriorate the signal-to-noise ratio.

The adaptation of existing nonselective heteronuclear correlation experiments to band-selective ones is straightforward and requires only a simple pulse calibration operation. A limitation of the proposed approach appears

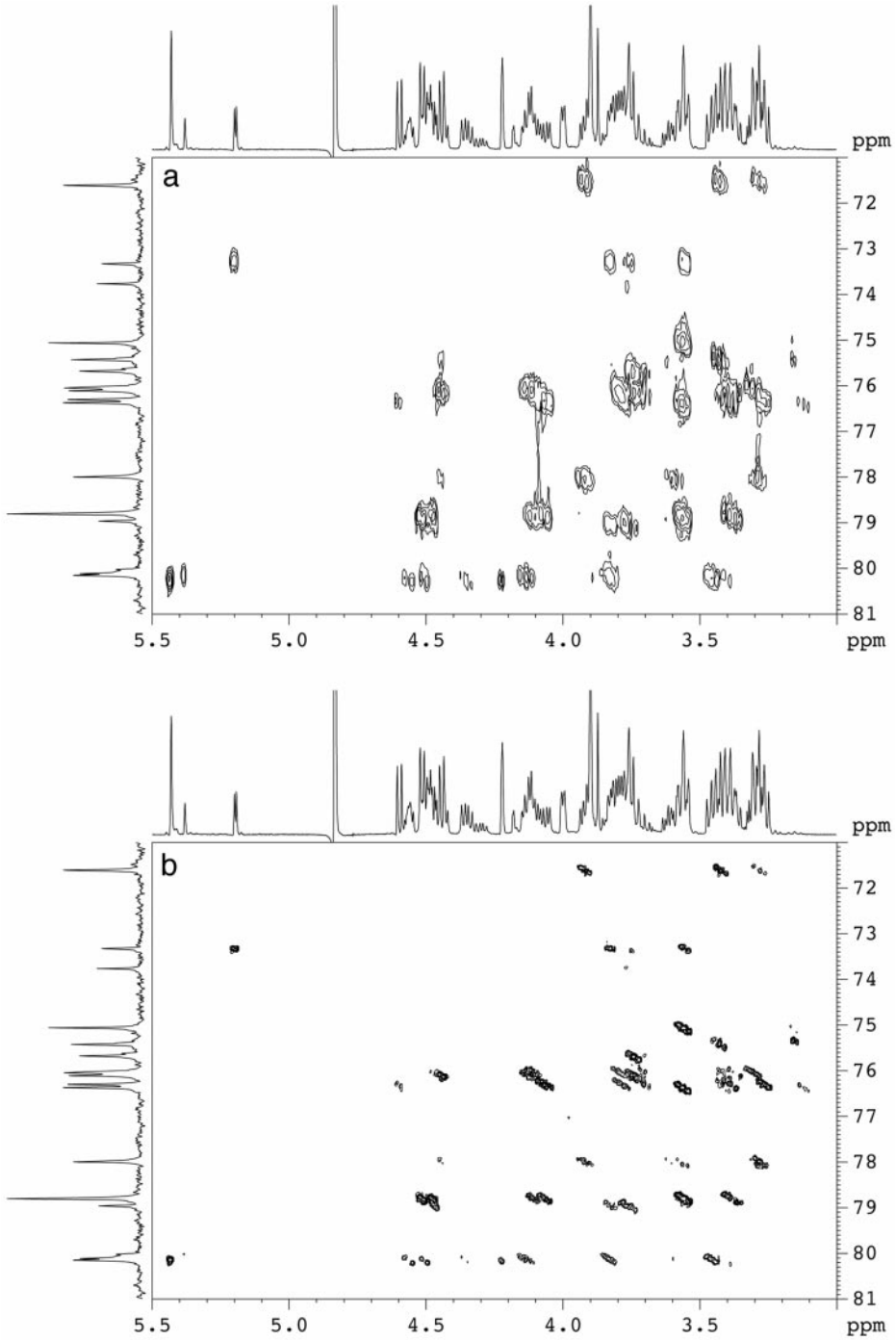

FIG. 5. (a) The $^{1}H–^{13}C$ HMBC spectrum of compound **1**. The total spectral width in F_1 is 130 ppm, with 512 t_1 increments (t_{1max} = 32 ms). Only the zone around 76 ppm is displayed. Gradient strengths G_1, G_2, and G_3 are 25, 15, and 20 G · cm^{-1}. Gradient pulses last 2 ms. The value of the delay τ' is 70 ms. Sixty-four scans were used per t_1 value, resulting in an overall recording time of 13.4 h. (b) The F_1-selective HMBC spectrum of compound **1**, recorded with the pulse sequence in Fig. 1d. The selective inversion is ensured by a RE-BURP pulse 2.5 ms long, covering a 16 ppm bandwidth. The total spectral width in F_1 is 20 ppm, with 256 t_1 increments (t_{1max} = 102 ms). Gradient strengths G_1, G_2, and G_3 are 15, −25, and 20 G · cm^{-1}. One hundred forty-four scans were used per t_1 value, resulting in an overall recording time of 14.9 h.

when attempting to use an excitation bandwidth of the order of magnitude (or less) of the direct heteronuclear coupling constant. The new pulse sequences described here should usefully complete the arsenal of techniques dedicated to structure solving of complex organic molecules by NMR.

ACKNOWLEDGMENTS

C.G. and C.L. thank the Région Champagne-Ardenne and the Département de la Marne (France) for financial support. We thank Dr. K. Plé for linguistic corrections.

REFERENCES

1. J.-M. Nuzillard and G. Massiot, Logic for structure determination, *Tetrahedron* **47,** 3655–3664 (1991).
2. J. J. Led and H. Gesmar, Application of the linear prediction method to NMR spectroscopy, *Chem. Rev.* **91,** 1413–1426 (1991).
3. V. A. Mandelshtam, H. S. Taylor, and A. J. Shaka, Application of the filter diagonalization method to one- and two-dimensional NMR spectra, *J. Magn. Reson.* **133,** 304–312 (1998).
4. R. Brüschweiler, J. C. Madsen, C. Griesinger, O. W. Sørsensen, and R. R. Ernst, Two-dimensional NMR spectroscopy with soft pulses, *J. Magn. Reson.* **73,** 380–385 (1987).
5. J. Cavanagh, J. P. Waltho, and J. Keeler, Semiselective two-dimensional NMR experiments, *J. Magn. Reson.* **74,** 386–393 (1987).
6. H. Oschkinat, C. Cieslar, T. A. Holak, G. M. Clore, and A. M. Gronenborn, Practical and theoretical aspects of three-dimensional homonuclear Hartmann–Hahn–Overhauser enhancement spectroscopy of proteins, *J. Magn. Reson.* **83,** 450–472 (1989).
7. B. Brutscher, J.-P. Simorre, and D. Marion, Optimization of multidimensional NMR using band-selective pulses, *J. Magn. Reson.* **100,** 416–424 (1992).
8. J.-M. Bernassau and J.-M. Nuzillard, Selective HMBC experiments using soft inversion pulses, *J. Magn. Reson. B* **103,** 77–81 (1994).
9. T.-L. Hwang and A. J. Shaka, Water suppression that works. Excitation sculpting using arbitrary waveforms and pulsed field gradients, *J. Magn. Reson. A* **112,** 275–279 (1995).
10. A. L. Davis, J. Keeler, E. D. Laue, and D. Moskau, Experiments for recording pure-absorption heteronuclear spectra using pulsed field gradients, *J. Magn. Reson.* **98,** 207–216 (1992).
11. E. O. Stejskal and J. E. Tanner, Spin diffusion measurements: Spin echoes in the presence of a time-dependent field gradient, *J. Chem. Phys.* **42,** 288–292 (1965).
12. R. R. Ernst, G. Bodenhausen, and A. Wokaun, "Principles of Nuclear Magnetic Resonance in One and Two Dimension," Oxford Univ. Press, New York (1987).
13. H. Geen and R. Freeman, Band-selective radiofrequency pulses, *J. Magn. Reson.* **93,** 93–141 (1991).
14. J.-M. Bernassau and J.-M. Nuzillard, Clean selective excitation of heteronuclear spin systems, *J. Magn. Reson. A* **104,** 212–221 (1994).
15. A. G. Palmer III, J. Cavanagh, P. E. Wright, and M. Rance, Sensitivity improvement in proton-detected two-dimensional heteronuclear correlation NMR spectroscopy, *J. Magn. Reson.* **93,** 151–170 (1991).
16. A. Bax and M. F. J. Summers, ^{1}H–^{13}C assignments from sensitivity-enhanced detection of heteronuclear multiple bond connectivity by 2D multiple quantum NMR, *J. Am. Chem. Soc.* **108,** 2093–2094 (1986).
17. J. J. Led, F. Abildgaard, and H. Gesmar, Phase correction of soft-pulse heteronuclear multiple-bond correlation spectra using backward linear prediction, *J. Magn. Reson.* **93,** 659–665 (1991).
18. J.-M. Bernassau and J.-M. Nuzillard, Enhancement of F_1-selective HMQC and HSQC experiments by field-gradient pulses, *J. Magn. Reson. A* **108,** 248–254 (1994).